An Attitude Control System for a Low-Cost Earth Observation Satellite with Orbit Maintenance Capability

Willem H Steyn
Yoshi Hashida
Surrey Space Centre
University of Surrey
Guildford, Surrey GU2 5XH
United Kingdom

Abstract. UoSAT-12 is a low-cost minisatellite built by Surrey Satellite Technology Ltd. (SSTL), it is amongst other objectives also a technology demonstrator for high performance attitude control and orbit maintenance on a future constellation of earth observation satellites. The satellite uses a 3-axis reaction wheel configuration and a cold gas propulsion system to enable precise and fast control of its attitude, for example, during orbit manoeuvres. Magnetorquer coils assist the wheels mainly for momentum dumping. This paper describes the various attitude control modes required to support: 1) the initial attitude acquisition phase, 2) a high resolution imager payload during pointing and tracking of targets, 3) the propulsion system during orbit manoeuvres. The specific attitude controllers and estimators used during these control modes are explained. Various simulation and in-orbit test results are presented to evaluate the performance and design objectives. To improve the control and estimation accuracy, on-board calibration and alignment procedures for the sensors and actuators are utilised. Some calibration results and the resulting improvement in accuracy from these procedures are shown.

Introduction

The UoSAT-12 minisatellite is not only the first low-cost minisatellite build by SSTL, but also the first satellite with 3-axis attitude determination and control capability. Another first is the cold gas and resistojet propulsion capability for orbit maintenance and attitude control. UoSAT-12 was launched in April this year in a 650 km circular, 64.5° inclination orbit. The main objectives of this mission is to demonstrate the minisatellite technology and enhance the payload technology at SSTL.

UoSAT-12 supports a wide range of sensors for attitude determination and a multi-channel GPS receiver for onboard orbit determination and accurate time synchronisation. The GPS receiver also has an experimental attitude determination capability, through baseline sensing of an array of 5 patch antennas. A redundant set of three 3-axis flux-gate magnetometers are used to measure the geomagnetic field vector in the satellite's body co-ordinates. These measurements are used to determine the magnetic coil torque vector and in combination with a magnetic field model to estimated the full attitude and angular rates of the satellite. Four 2-axis (azimuth and elevation) sun sensors measure the sun vector angle to high accuracy. During the nominal nadir pointing attitude mode, small pitch and roll angles can be measured with a 2-axis infrared horizon sensor. The highest attitude measurement accuracy is obtained from a dual set of opposite looking star sensors. These are used to track stars down to a visible magnitude of 6.0 m_v. The sensors supply star measurement vectors and matched star catalogue vectors at a rate of once per second to an attitude and rate estimation filter. A solid state angular rate sensor is mounted in one axis of the satellite to flight qualify the sensor for future mission. Table 1 lists all the sensors used on UoSAT-12 for attitude determination and their most important characteristics.

Twelve magnetorquer coils are positioned within the satellite to give some level of redundancy and to deliver full 3-axis magnetic dipole moment control. These coils are controlled by using dual polarity current pulse width control to deliver the required averaged level of magnetic moment per sample period. The magnetorquers are used for:

- Detumbling of body angular rates after launch
- Momentum dumping of the reaction wheels
- Momentum maintenance on the momentum wheel during Y-spin stabilisation
- Nutation damping during spin stabilisation

- Libration damping and yaw spin/phase control after deployment of a backup gravity gradient boom

Three momentum/reaction wheel subassemblies are mounted in a 3-axis configuration to enable full control of the attitude or angular momentum of the satellite. One wheel is a space qualified wheel from Ithaco and mounted in the structural Y-axis direction to have higher reliability when the pitch momentum bias control mode is used. The SSTL manufactured wheels, destined to be space qualified on UoSAT-12, are mounted in the structural X and Z-axis direction. The wheels are used for the following control functions:

- Full 3-axis pointing and slow slew manoeuvres during imaging
- Nadir, sun or inertial pointing of the payloads by using angular momentum stiffening
- Near minimum-time Euler-axis rotations for quick attitude manoeuvres
- Fast spin-up or spin-down of the satellite body e.g. barbecue mode of the solar arrays
- Cancellation of the disturbance torque caused by the propulsion system during orbit control
- Thruster and moment of inertia calibration

UoSAT-12 is fitted with a single N_2O resisto-jet thruster for orbit maintenance and 10 cold gas nitrogen thrusters for orbit or attitude control. The resisto-jet is aligned to the centre of mass of the satellite to give small attitude disturbances. Some cold gas thrusters can be used in pairs to limit the attitude disturbance torque during orbit control manoeuvres. The propulsion system can be used for the following functions:

- Full 3-axis rough pointing and fast slew control
- Drag compensation of the satellite's orbit
- Orbit shaping to demonstrate constellation control
- Wheel momentum dumping/maintenance

Table 2 lists the various actuators used on UoSAT-12 for attitude and orbit control and their respective characteristics.

Table 1: Attitude and orbit determination sensors on UoSAT-12

	Magnetometer	*Sun Sensors*	*Horizon Sensor*	*Star Sensor*	*Rate Gyro*	*GPS*
Manufac-turer	SSTL (2) Ultra (1)	SSTL	Servo - MiDES SSTL I/F	SSTL	BEI SSTL I/F	SSTL
Quantity	3 units	4 x 2-axis	1 x 2-axis	2 units	1 unit	1 unit
Type	Flux Gate	Slit & Photo cell	IR pyro array & chopper	CCD matrix	Gyrochip	Mitel Chip set
Range	+/- 60 μTesla	+/- 50°	+/- 5.5°	14.4° x 19.2° +1.0-6.0 m_v	+/- 5 °/s	24 Channels 4 Antennae
Accuracy	30 nTesla (3σ)	0.2° (3σ)	0.06° (3σ)	0.02° (3σ)	0.02 °/s	50 m (1σ)
Power	< 0.8 W	< 0.1 W	2.8 W	4 W	1.4 W	5-7 W

Table 2: Attitude and orbit control actuators on UoSAT-12

	Magnetorquers	*Reaction/Momentum Wheels*	*Propulsion System*
Manufacturer	SSTL	SSTL (2) Ithaco (1)	SSTL & Polyflex
Quantity	8 x PCB 4 x Wire coils	3 units (X/Y/Z)	10 x N_2 CG thrusters 1 x N_2O Resisto-jet
Type	Air Core	Brushless DC motor Dry lubricated bearings	4 Bar Cold Gas, N_2O plus 100 W heater
Operation Range	X/Y = +/- 14.2 Am^2 Z = +/- 13.3 Am^2	+/- 4 Nms @ +/- 5000 rpm +/- 0.02 Nm max.	Thrust: 0.1 N (CG) 0.125 N (R-jet) Delta-V: 14 m/s (CG) 9.7 m/s (R-jet)
Power	20 W max. (80 % duty cycle)	2.8 - 14.6 W (zero to max. accel.)	3 W (CG) 100 W (R-jet)
Operation Accuracy	PWM controlled 20 msec minimum ulse	Speed controlled +/- 1 rpm	PWM controlled > 10 msec pulse (CG) > 600 sec pulse (R-jet)

Initial Attitude Acquisition

After separation from the launch vehicle, the satellite can be tumbling at a unknown rate. A simple B-dot[1] rate damping controller requiring only a Y-axis magnetic moment is used. This controller will reduce the X- and Z-axis angular rates and align the spacecraft's Y-axis to the orbit normal. No attitude or rate information is explicitly required. The controller is implemented by measuring the magnetic field vector at regular intervals and the M_y magnetorquer is fired for short periods at the correct polarity, depending on the angular rate of the magnetic field vector:

$$M_y = K_d \dot{b} \quad , \quad b = \arccos\left(\frac{B_y}{\|\mathbf{B}\|}\right) \tag{1}$$

with K_d a constant gain parameter.

The next step will be to simultaneously control the Y-axis rate of the spacecraft's body to a certain reference value. This will bring the satellite to a Y-Thomson[2] mode of stabilisation. This can be done by using a X-axis magnetic moment (or alternatively the Z-axis). The magnetorquer pulse duration and polarity depends on the angular rate error and the polarity of the Z-axis component of the magnetic field vector (or alternatively the X-axis):

$$M_x = K_s\left(w_{yo} - w_{yo-ref}\right)\mathrm{sgn}\left(B_z\right) \tag{2}$$

with K_s a constant gain parameter, w_{yo} the orbit referenced angular rate of the spacecraft's body can be estimated from a simple pitch filter or a Kalman rate filter[3].

The pitch filter is reasonably accurate once the satellite is in a pure Y-Thomson spin (i.e. small roll and yaw assumption). This filter will determine both the orbit referenced pitch angle q and rate $\dot{q}$ ($\approx w_{yo}$) using the magnetometer measurements and the modelled IGRF[4] geomagnetic field vector. The filter is based on a double integrator model of the decoupled pitch axis of the spacecraft's dynamics:

$$\ddot{q} = N_y / I_{yy} \tag{3}$$

with N_y the total torque applied and I_{yy} the moment of inertia (MOI) around the spacecraft Y-axis. The discrete state space model for a sampling period of Δt can then be written as:

$$\begin{bmatrix} q(k+1) \\ \dot{q}(k+1) \end{bmatrix} = \begin{bmatrix} 1 & \Delta t \\ 0 & 1 \end{bmatrix} \begin{bmatrix} q(k) \\ \dot{q}(k) \end{bmatrix} + \begin{bmatrix} \Delta t^2 / 2I_{yy} \\ \Delta t / I_{yy} \end{bmatrix} N_y(k) \tag{4}$$

The measurement equation assuming a pure Y-spin:

$$q = \tan^{-1}\left\{\frac{-b_x b_{zo} + b_z b_{xo}}{b_x b_{xo} + b_z b_{zo}}\right\} \tag{5}$$

The b_{io} and b_i terms are normalised modelled (orbit referenced) and measured geomagnetic field vector components, as only the direction of the vectors is important. Equations (4) and (5) are then used in a discrete second order state to determine the filtered pitch angle and rate values.

A Kalman type rate filter is also implemented during the initial tumbling phase to determine all the angular body rates from magnetometer measurements only. The detail of this filter is explained in Reference 3. The main advantages of this rate estimator are: 1) no orbit propagator and hence no IGRF computation is required (fast sampling possible), 2) the filtering algorithm is very simple and has low computational demand, 3) it is robust against modelling errors and it does not diverge. The main disadvantage is that rate estimation errors similar in size to the orbit angular rate w_o (mean motion) will occur.

After the satellite has been fully detumbled and brought to the reference Y-Thomson state, a Y-axis momentum wheel is used to absorb the body momentum and stabilise the satellite into a fixed nadir pointing attitude (zero roll, pitch and yaw). The first phase of this manoeuvre is to ramp the Y-wheel momentum (speed) to close to the initial body momentum. This will slow down the Y-axis body rate. When the target wheel speed is reached, it is kept constant and the satellite body allowed to drift towards its nadir pointing attitude. When the pitch angle (estimated by the pitch filter) becomes less than ± 20° from nadir a closed loop PD-type wheel pitch attitude controller is enabled:

$$N_{wy} = K_d \dot{q} + K_p\left(q - q_{ref}\right) \quad \text{and} \quad \left|N_{wy}\right| \le N_{w\_\max}$$
$$w_{wy} = \int N_{wy}\,\mathrm{d}t \Big/ J_{wheel} \quad \text{and} \quad \left|w_{wy}\right| \le w_{w\_\max} \tag{6}$$

where K_p and K_d are the PD controller gains, N_{wy} and $N_{w\_\max}$ are the Y-wheel required and maximum torque values, w_{wy} and $w_{w\_\max}$ are the Y-wheel reference and maximum speed values, and J_{wheel} is the wheel MOI.

The reference pitch angle q_{ref} is zero for the nadir pointing case, but can be any angle in the Y-axis stabilised mode. To maintain the wheel momentum at a certain reference level and to damp any nutation in roll and yaw, a magnetorquer cross-product[5] control law is utilised:

$$\mathbf{M} = \frac{\mathbf{e} \times \mathbf{B}}{\|\mathbf{B}\|} \tag{7}$$

with,

$$\mathbf{e} = \begin{bmatrix} K_x w_{xo} \\ K_y \left(h_{wy} - h_{wy-ref} \right) \\ K_z w_{zo} \end{bmatrix} \tag{8}$$

K_i is the controller gain constants, w_{io} is the orbit reference angular rates and h_{wy} and $h_{wy\text{-}ref}$ is the Y-wheel angular momentum measurement and reference values. The orbit reference angular rates in Eq. (8) are obtained from a full state (attitude and rate) Extended Kalman filter (EKF) for improved accuracy above the Rate Kalman filter mentioned previously. This filter will be described in the next paragraph.

Figures 1 and 2 shows the simulation performance of the B-dot controller, Rate Kalman filter and Pitch filter during the initial detumbling period. The initial orbit referenced angular rate vector is $\boldsymbol{\omega}_B^O = \begin{bmatrix} 1 & 0 & 2 \end{bmatrix}^T$ °/s. The rate damping controller of Eq.(1) is immediately enabled. After one orbit (6000 seconds) the Rate Kalman filter is enabled and one orbit later (12000 seconds) the Y-spin controller of Eq.(2) is started. The Y-axis body rate is controlled towards -1 °/s. The target rate is almost reached within 1 orbit. The Pitch filter is then enabled and the improved Y-rate estimation from the Pitch filter is used for the next 2 orbits.

At the start of the 4th orbit (18000 seconds) the Y-wheel is ramp to a momentum of -0.8 Nms using an open-loop strategy. The Y-body rate is slowed from -0.9 °/s to +0.2 °/s as the satellite's body momentum is absorbed by the wheel. After 1000 seconds the wheel reached its target of -1000 rpm (-0.8 Nms) and the speed is kept constant to allow the pitch angle to drift towards the nadir direction. During the 4th orbit the spin damping controller of Eq.(1) is activated to damp any nutation motion. When the pitch angle is within 20° from nadir, the Pitch wheel controller of Eq.(6) and the Cross-product wheel momentum controller of Eqs.(7,8) are enabled. Within a few minutes the pitch angle of the satellite is zeroed and the satellite is now Y-momentum wheel stabilised. At the start of the 5th orbit the full state EKF is initialised, but the Pitch wheel controller is still using the Pitch filter estimates until the EKF has converged. After EKF convergence, nutation damping is enabled to reduce the roll and yaw errors (see Eq.(8) for x and z components of error vector). The accumulated magnetorquer on-time during the wheel commis-sioning phase is slightly more than 600 seconds.

Figure 3 shows the simulated performance of the Y-wheel and Cross-product magnetorquer controller for initial pitch, roll and yaw errors. The initial roll and yaw errors are +10° and -10° respectively and the Y-wheel has an angular momentum of –0.8 Nms (-1000 rpm). The satellite is in an uncontrolled nutation motion and the pitch angle drifts during the first orbit. The full state EKF is also allowed to converge during the first orbit. At the start of the second orbit, the Pitch wheel (Eq.(6)) and the Cross-product (Eqs (7,8)) controllers are enabled. Within approximately one orbit all the attitude errors are removed and the satellite is in an accurate nadir pointing state. The accumulated magnetorquer on-time during this attitude control effort is slightly less than 1000 seconds.

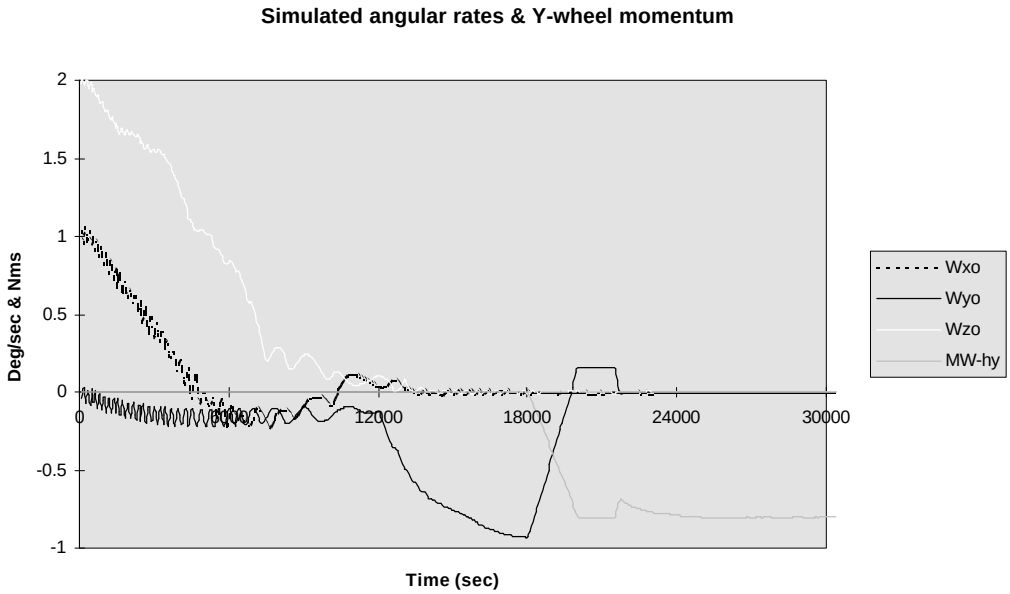

Figure 1 Simulation of flight software from detumbling to Y-momentum control

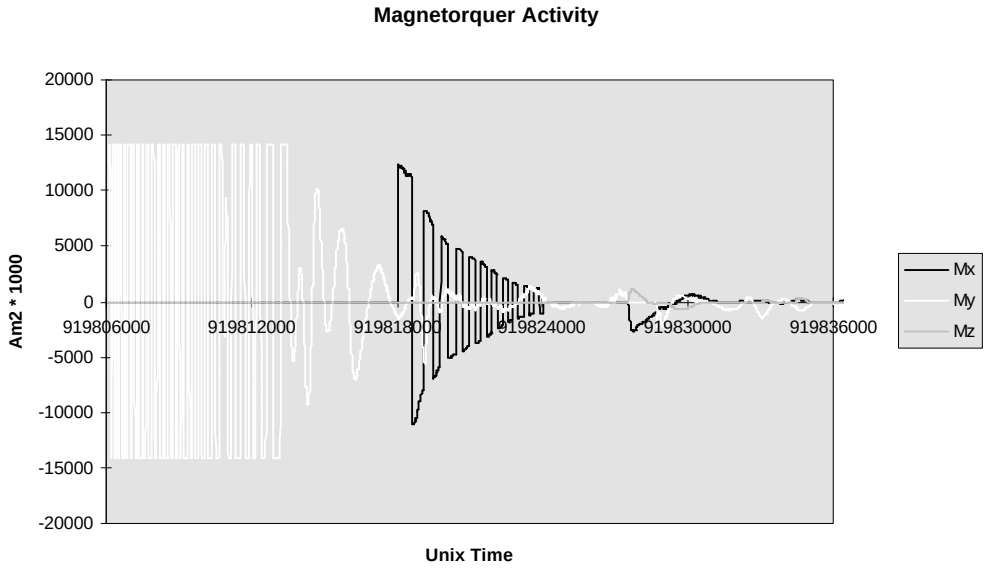

Figure 2 Simulated magnetorquer activity from detumbling to Y-momentum control

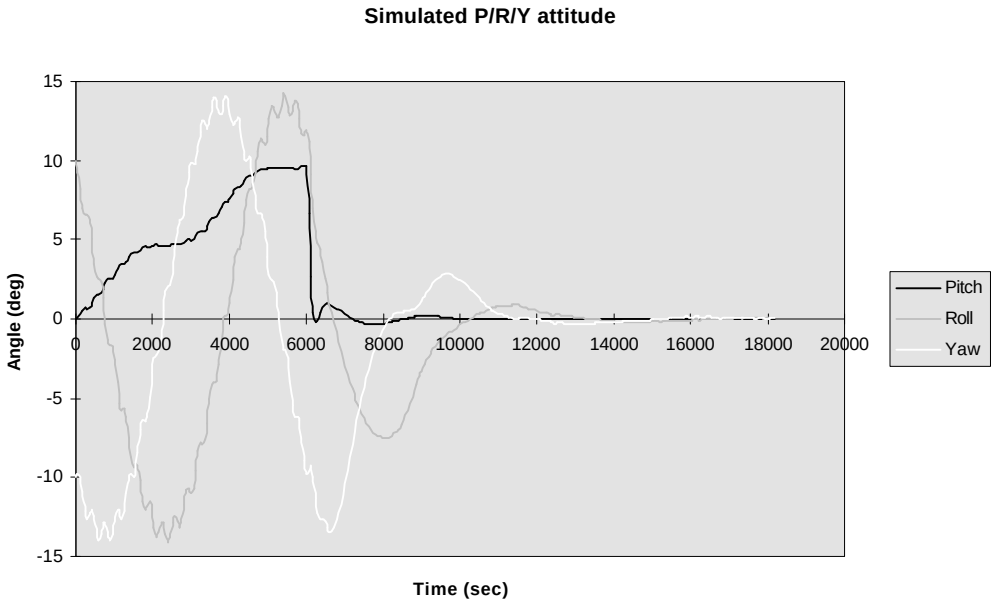

Figure 3 Simulated attitude during nutation damping in Y-momentum mode

Full 3-axis Attitude Control

To support target pointing and tracking during imaging a full 3-axis zero-bias reaction wheel control system is employed. Since the attitude can be controlled in any direction, a quaternion based Extended Kalman filter[6] (EKF) is implemented. This filter takes measurement vectors (in the body frame) from all the attitude sensors and by combining them with corresponding modelled vectors (in a reference frame), estimates the attitude and angular rate values of the satellite. The 7-element discrete state vector to be estimated, is defined as:

$$\mathbf{x}(k) = \left[\boldsymbol{\omega}_B^{I\,T}(k) \quad \mathbf{q}^T(k) \right]^T \qquad (9)$$

with $\boldsymbol{\omega}_B^I$ the inertial referenced angular rate vector and $\mathbf{q}$ the orbit referenced quaternion vector. The innovation used in the EKF is the vector difference between the measured body referenced vector and a modelled orbit referenced vector, transformed to the body frame by the estimated attitude transformation matrix:

$$\mathbf{e}(k) = \mathbf{v}_{meas}(k) - \mathbf{A}\left[\hat{\mathbf{q}}(k)\right]\mathbf{v}_{orb}(k) \qquad (10)$$

where,

$$\mathbf{v}_{meas}(k) = \mathbf{B}_{meas}(k) \big/ \left\|\mathbf{B}_{meas}(k)\right\|$$

$$\mathbf{v}_{orb}(k) = \mathbf{B}_{orb}(k) \big/ \left\|\mathbf{B}_{orb}(k)\right\|$$

for the magnetometer measurement and IGRF modelled vectors.

The same method is applied for all the attitude sensors, to supply a measurement and modelled vector pair to the filter when a valid sensor output is received. Depending on the sensor type, various measurement noise covariance values are used in the Kalman filter put different weight factors on the less accurate (magnetometer) and the more accurate (e.g. star sensor) innovations.

Pointing and tracking controllers are used to obtain accurate and low distortion images. Large angular slew manoeuvres are optimised using a near minimum time eigenaxis rotation algorithm[7].

The globally stable quaternion feedback control law of Wie[8] was modified to be implemented on UoSAT-12 as an orbit referenced pointing control law:

$$\mathbf{N}_{wheel} = \mathbf{K}\mathbf{q}_{vec} + \mathbf{D}\boldsymbol{\omega}_B^O - \boldsymbol{\omega}_B^I \times \left(\mathbf{I}\boldsymbol{\omega}_B^I + \mathbf{h}\right) \qquad (11)$$

where,

$\mathbf{K} = k\mathbf{I}$, $\mathbf{D} = d\mathbf{I}$ {Scaled MOI matrices},

$\mathbf{q}_{vec} = \left[q_{1e} \quad q_{2e} \quad q_{3e}\right]^T$ {Vector part of error quaternion}

The error quaternion $\mathbf{q}_e$ is the quaternion difference between the commanded quaternion $\mathbf{q}_c$ and the current satellite quaternion.

The tracking control law is used when a reference rate profile is implemented:

$$\mathbf{N}_{wheel} = \mathbf{K}\mathbf{q}_{vec} + \mathbf{D}\left(\boldsymbol{\omega}_B^O - \boldsymbol{\omega}_{ref}\right) - \mathbf{I}\dot{\boldsymbol{\omega}}_{ref} - \boldsymbol{\omega}_B^I \times \mathbf{h} \quad (12)$$

where,

$\boldsymbol{\omega}_{ref}$ = target reference angular rate vector

Momentum management of the wheels are done using a simple cross-product controller:

$$\mathbf{M} = K_m \left(\mathbf{h} \times \mathbf{B}_{meas}\right) / \left\|\mathbf{B}_{meas}\right\| \quad (13)$$

with,

K_m = controller gain constant

In-Orbit Commissioning

UoSAT-12 was launched on the 21st of April 1999 from the Baikonur Cosmodrome in Khazakstan. The initial telemetry of the magnetometer indicated a tumbling rate of about 2 °/s. The next day the ADCS software was loaded on the 186-OBC and the Rate Kalman filter confirmed the initial tumbling rate to be mainly around the Y-axis. The first estimated rates can be seen in Figure 4. This result confirmed the slightly higher Y-axis MOI and the cross-products of inertia.

On the 24th of April the detumbling sequence commence. Initially only the M_y torquer (Eq.(1)) was used to dump the X and Z-axis angular rates, then the M_x torquer (Eq.(2)) was enabled to control the Y-axis rate towards the Y-Thomson reference rate of -1 °/s. Figure 5 and 6 show the first in-flight detumbling results, the first orbit using only M_y and the second orbit adding M_x to also control the Y-axis rate. After 2 orbits the body angular momentum of UoSAT-12 was almost completely dumped. The magnetorquer controller was left running for 2 more orbits until the satellite was in the required Y-Thomson attitude. The cross-products of inertia prevented the satellite to reach the target rate exactly and the true Y-rate estimated was approximately -0.8 °/s with small residual X and Z-rates of less than 0.2 °/s.

The Y-wheel was polarity tested and the magneto-meter re-calibrated the next day (25th April). On the 26th April the Y-wheel was used the first time to stop the Y-body spin. The wheel speed was ramp to -1000 rpm in 1000 seconds and the body rate changed from -0.8 °/s to a slow positive rotation of 0.3 °/s. The wheel speed was held at a constant speed until the estimated pitch angle drifted to within 20 degrees from nadir. The closed loop wheel controller (Eq.(6)) was then enabled and the pitch angle controlled to the zero reference within a few seconds. Figures 7 and 8 present the results as logged by the on-board ADCS task.

The next few weeks the nadir pointing performance of the Y-momentum control mode was improved by calibrating and aligning the magnetometer used for attitude determination in the EKF. Figure 9 shows the attitude during 5 orbits on the 30th of April. The magnetometer calibration was then improved using an off-line least square procedure to estimate the offsets and 3x3 gain matrix for scale factor and misalignment correction:

$$\mathbf{B}_{calib}(k) = \mathbf{G}(k)\mathbf{B}_{meas}(k) + \mathbf{H}(k)$$

with,

G = scale factor/misalignment matrix
H = offset (bias) vector

Figure 10 shows the attitude control results during 5 orbits after calibration on the 10th of May. The mean and standard deviation values for the attitude angles before and after calibration are summarised in Table 3. The magnetometer calibration has reduced the deviation in all axes by more than 100%. The attitude errors still present must be caused by magnetometer disturbances (from onboard environment), IGRF modelling errors and Y-wheel misalignment. The attitude estimation errors will only improve further once the more accurate sensors (e.g. star sensor) are included in the EKF.

Table 3: Attitude performance before and after magnetometer calibration

	Mean (28/4)	*Std-Dev (28/4)*	*Mean (10/5)*	*Std-Dev (10/5)*
Roll (deg)	0.78	2.21	-0.35	0.39
Pitch (deg)	-0.04	0.29	-0.05	0.15
Yaw (deg)	0.78	1.77	0.72	0.59

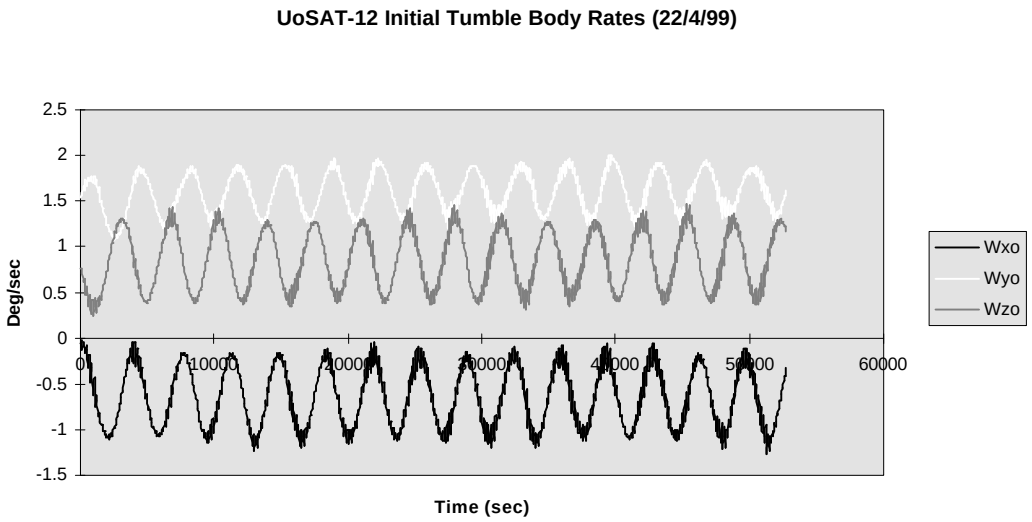

Figure 4 Initial orbit referenced body rates of UoSAT-12 before detumbling

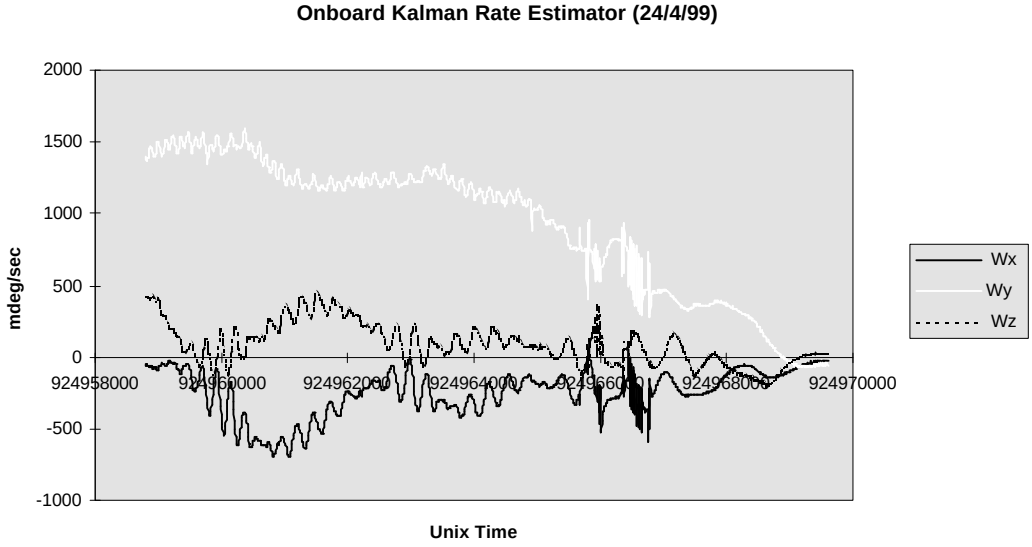

Figure 5 Estimated angular rates during detumbling of UoSAT-12

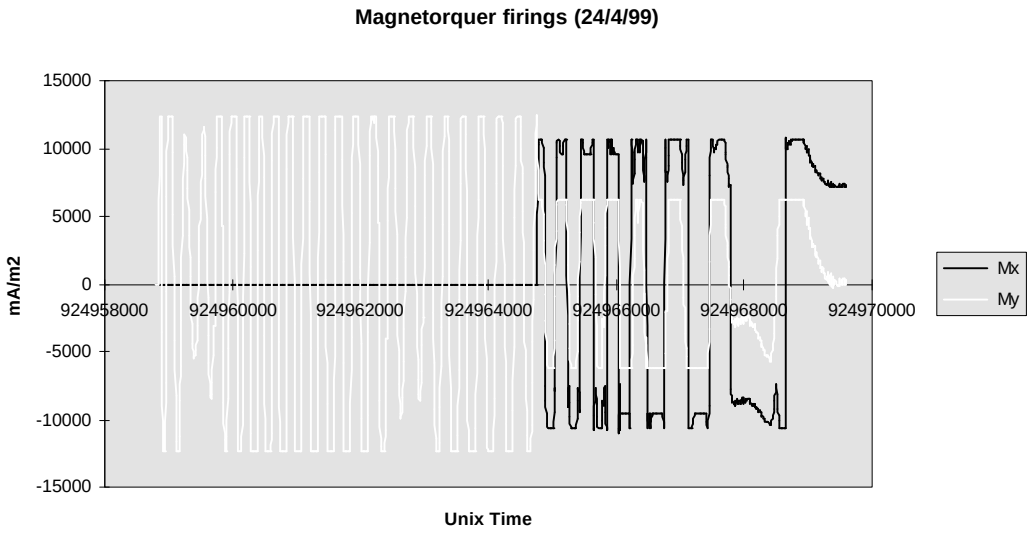

Figure 6 Magnetorquer activity during UoSAT-12 detumbling

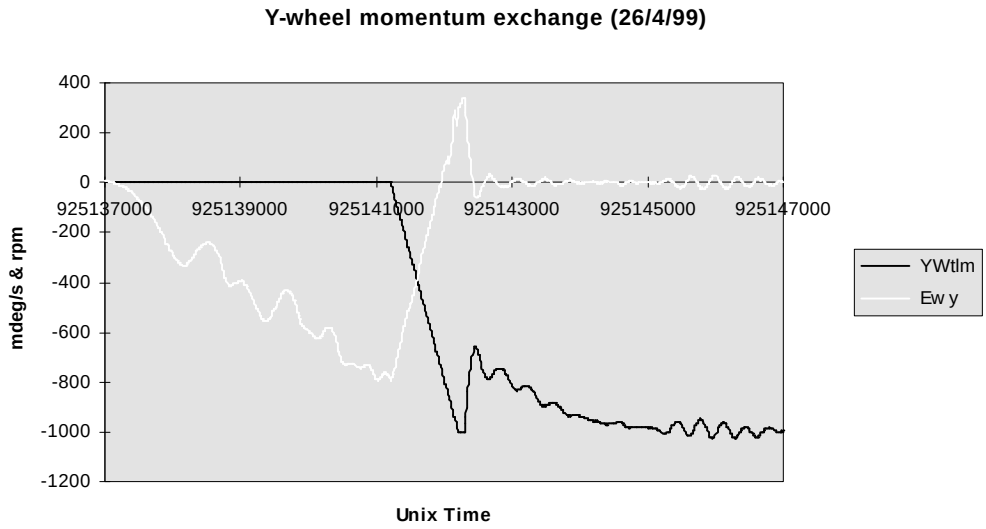

Figure 7 Momentum exchange during Y-spin to nadir pointing control

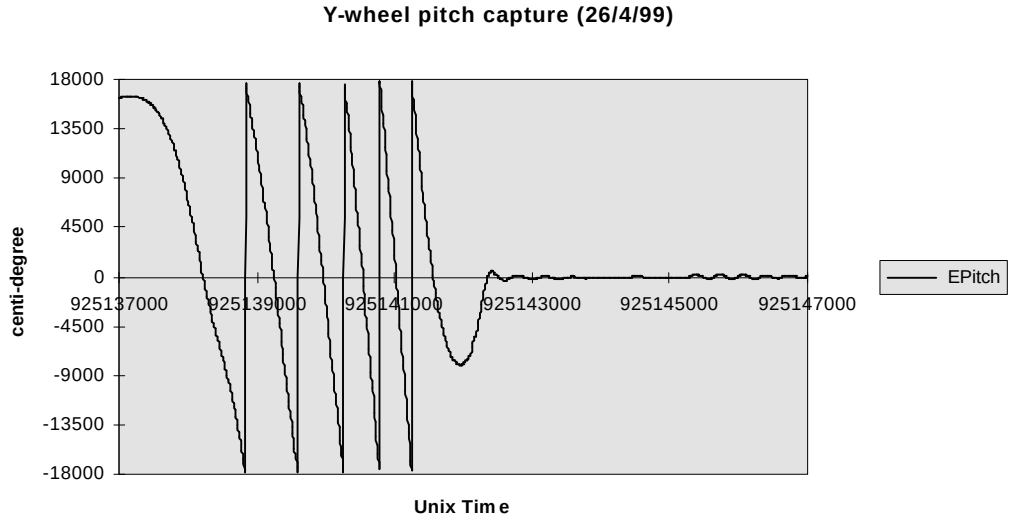

Figure 8 Pitch angle during Y-Thomson to nadir pointing control

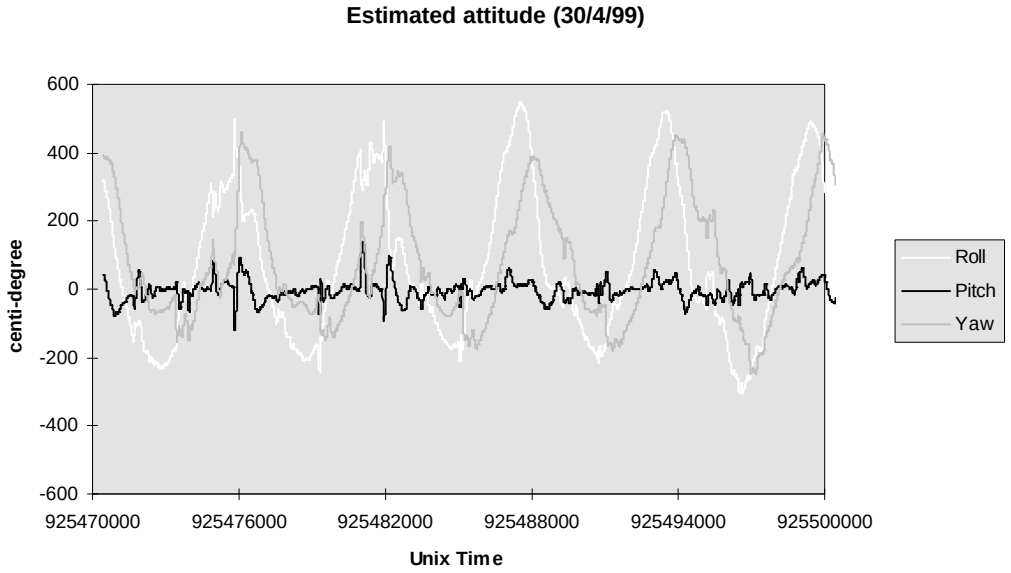

Figure 9 Initial attitude performance during Y-momentum control

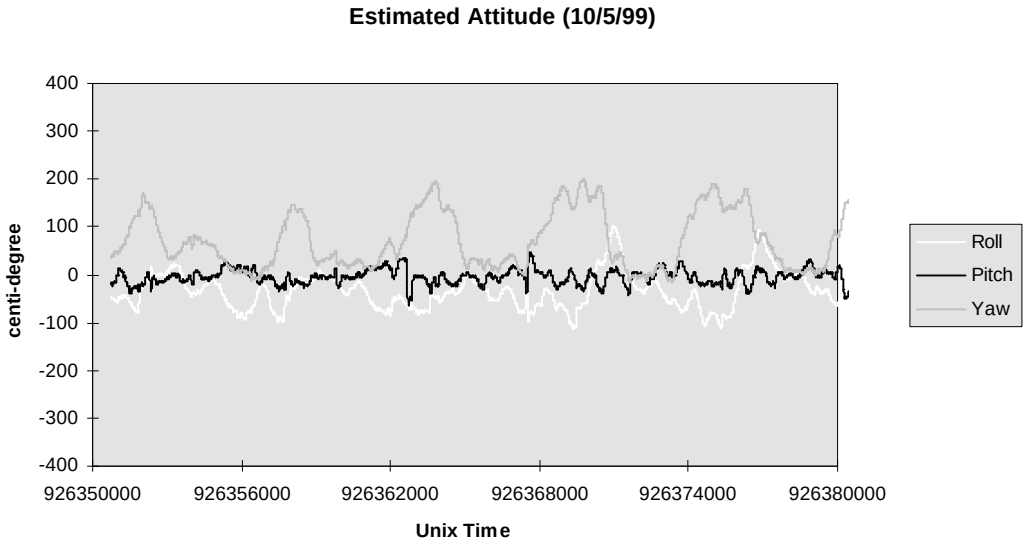

Figure 10 Attitude performance after magnetometer alignment and calibration

In-Orbit Reaction Wheel Control

UoSAT-12 was next fully 3-axis stabilised in zero momentum mode using the SSTL-1 and SSTL-2 reaction wheels for the Z- and X-axis respectively and the Ithaco wheel in the Y-axis. This control mode has been entered on the 9th of June when the Y-wheel momentum was dumped completely and the X and Z wheels activated. The event is captured in Figure 11. A magnetometer and the MiDES horizon sensor were used to supply vector measurements to the onboard EKF estimator. The main feature of this ADCS mode is that it can control the satellite's attitude accurately in all axes. However, the limited FOV of the horizon sensor restricts the controller to maintain small roll and pitch angles at all time (nadir pointing). The yaw angle can be controlled freely to any reference value and even a slow Z-rotation is possible (< 0.2°/s). To remove the attitude control restriction on the roll and pitch angles, the sun sensor measurements must be included in the EKF (only possible during the sunlit part of the orbit), or ultimately the star sensor will be used once it is fully commissioned.

Table 4 and Figures 12 to 14 summarise the control performance over a period of 11 hours on the 16th of June. The pitch and roll pointing errors experienced

are very small, the 1-σ deviation is 0.13° and the maximum peaks during this period less than 0.5°. The yaw error is worse (1-σ deviation is 0.62°) due to a lack of accurate yaw information close to the polar region. The reason being the use of the magnetometer as the only source of yaw information to the EKF estimator. Yaw control peaks of up to 3 degrees are only experienced for short periods at the maximum latitude extremes of each orbit. The reaction wheels are running mostly below 20 rpm and the magnetorquer peaks are 2.5 % of the saturation limit. The magnetorquers are used exclusively to dump any wheel momentum build-up (see Eq.13).

Table 4: Zero momentum ADCS performance

	Roll (deg)	*Pitch (deg)*	*Yaw (deg)*	w_x *(mdeg/s)*	w_y *(mdeg/s)*	w_z *(mdeg/s)*	*RW-X (rpm)*	*RW-Y (rpm)*	*RW-Z (rpm)*
Std-Dev	0.13	0.13	0.62	2.0	1.8	5.9	9.3	5.7	13.4
Mean	-0.05	-0.02	0.08	0.4	-60.6	-0.9	0.7	-5.0	5.1

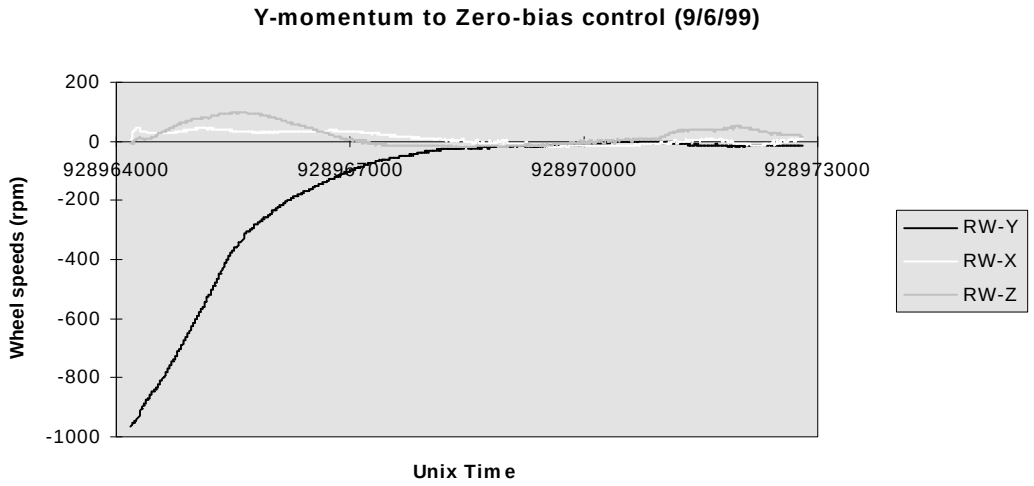

Figure 11 Wheel speed profiles during Y-momentum dumping

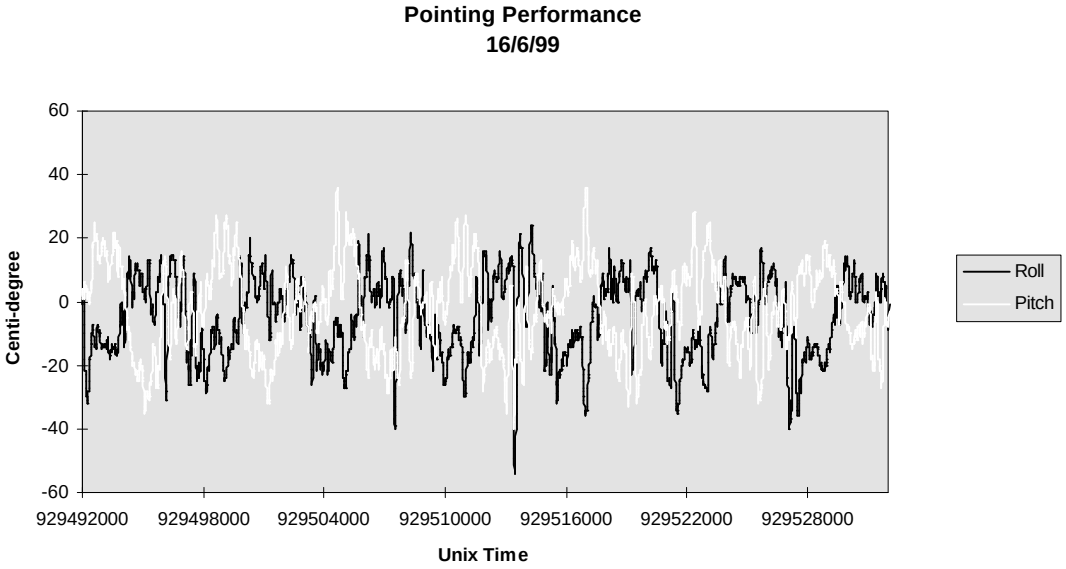

Figure 12 Roll and pitch pointing during zero-bias 3-wheel control

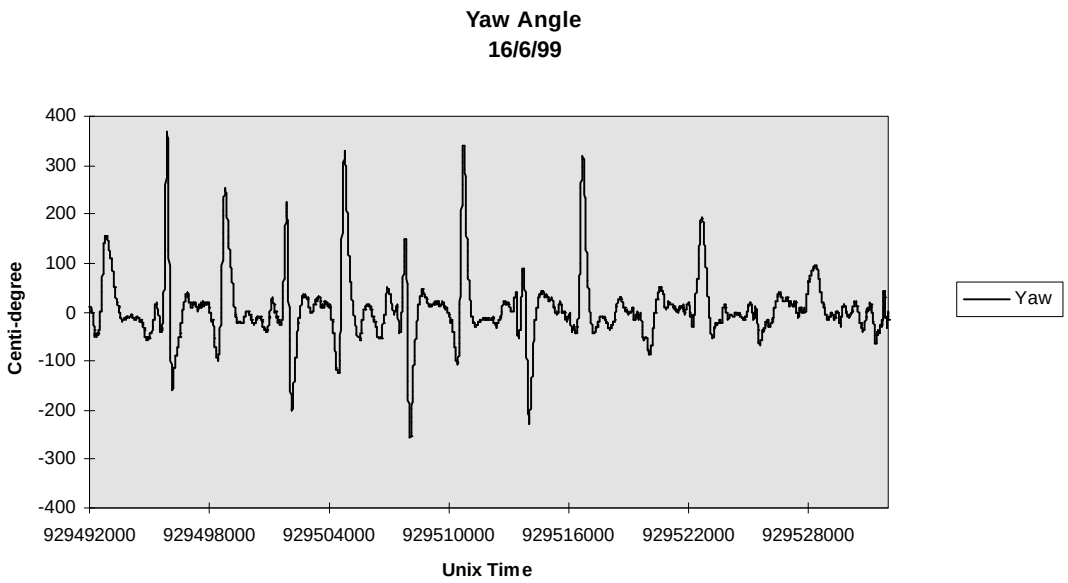

Figure 13 Yaw angle performance during zero-bias 3-wheel control

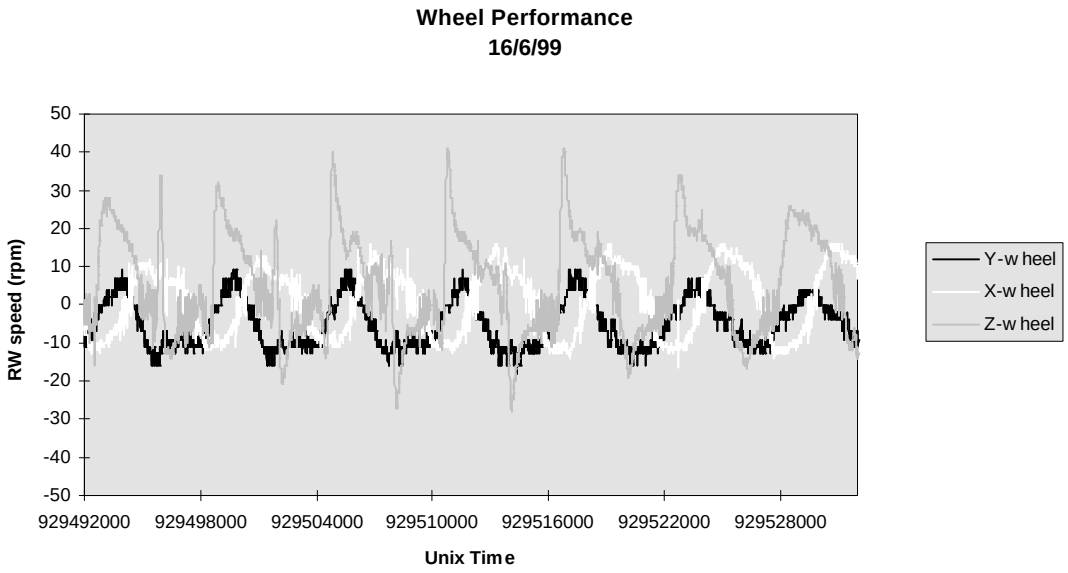

Figure 14 Wheel speed performance during zero-bias 3-wheel control

Orbit Control Experiments

Orbit control experiments have not been implemented yet. However, the plan is to change UoSAT-12's orbit to frozen orbit conditions, using the propulsion systems as described in the Introduction paragraph

Because the inclination angle of UoSAT-12 is near to the so-called critical inclination (*i*) which satisfy the condition: $4-5\sin^2 i = 0$, the frozen condition for UoSAT-12 is now inverted, i.e. the frozen argument of perigee is not 90 degrees, but 270 degrees. That is caused by the sign change of the long periodic perturbation parameter due to the higher order terms which has a denominator of $4-5\sin^2 i$, whereas the J_3/J_2 term does not. Assuming the current UoSAT-12 inclination of 64.5 degrees, the required eccentricity to freeze the orbit is about 0.0021.

Orbit determination will be carried out autonomously onboard, assuming GPS measurements are obtainable. Two types of onboard orbit estimators are used, depending upon the available processing power

and the required accuracy. One is based upon an analytic formulation of the perturbed orbit, which has a small code size and requires a low computational demand. Sub- kilometre accuracy can be expected for about an one week period of propagation. The other is a highly accurate estimator which uses a numerical integration technique. The numerical integrator approach is normally costly on processing time, because not only the orbital state but also the state transition matrix have to be integrated. Integration using a Symplectic method[9] is used to obtain high accuracy but also to keep the processing time as low as possible. The great advantage, however, when using this integration method, is that the potential function can be expanded to any order and degree of the gravitational model (WGS84 defined coefficients up to 36 order and degree are used). The expected accuracy will not exceed a hundred metres in all axes, which is about the same magnitude as the intentional error imposed on the GPS measurements.

The expected performance of the high-accuracy orbit determination function has already been demonstrated. GPS measurements have been downloaded from UoSAT-12 and processed on ground for verification prior to the actual onboard use. GPS measurements were sampled every 10 seconds and logged on the 18th of June. Modelled geo-potential terms were used (36 order and 36 degree) to estimate the orbit. In Figure 15, the history of the radial error between the original GPS fixed versus filtered position is shown. The errors in along- and cross-track directions are smaller than those in the radial direction. The statistical values for these errors are presented in Table 5:

Table 5: GPS versus Estimated position errors

	Along	*Cross*	*Radial*
Mean (m)	-0.469	2.07	4.83
Std-Dev (m)	21.3	22.1	40.5

The experimental orbit control experiment will use both the N_2 cold gas thrusters and N_2O resistojet.

It is required to change both the eccentricity (*e*) and the argument of perigee (*w*) in order to move the satellite into a frozen orbit. Propulsion system constraints and attitude maintenance requirements, will force multiple small burns for the orbit transfer. This, however, allows enough time for correction of any induced errors during the orbit manoeuvre.

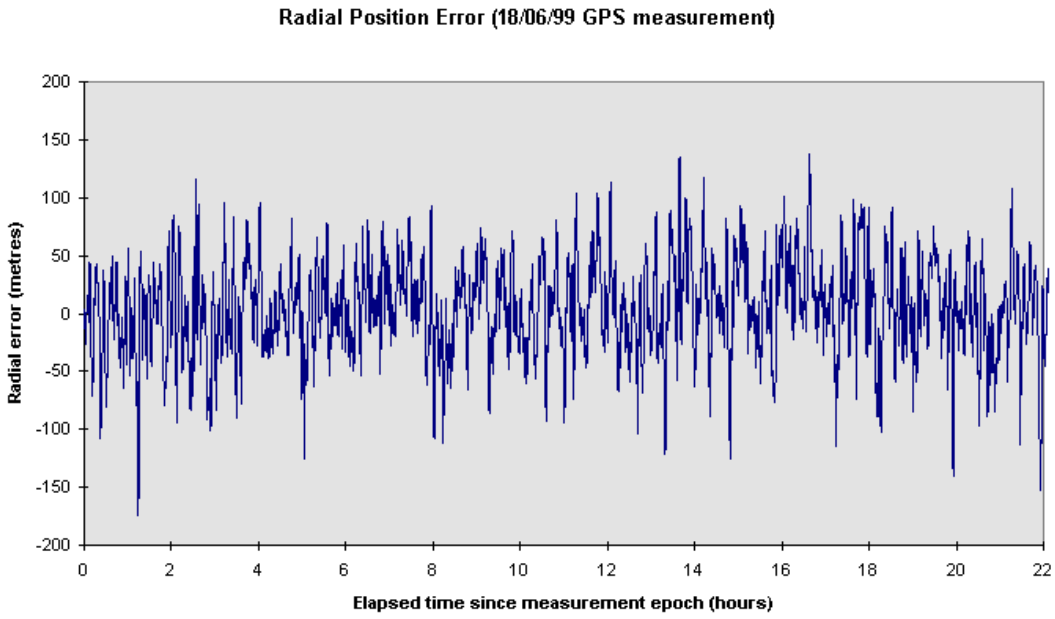

Figure 16 Radial position error of the GPS versus the estimator output of UoSAT-12's orbit

Conclusions

The first in-orbit results from the UoSAT-12 ADCS proved to be close to the performance of the pre-launch simulation predictions. Although inclusion in the EKF of the high accuracy star sensor measurements and proper alignment of all the sensors plus actuators have not been completed by the time this paper was written, good pointing accuracy has already been achieved.

Full 3-axis control using 3 reaction wheels under zero momentum bias gave the best pointing performance as expected. The wheel speed peaks during this control mode were only a few tens of rpm which will not only extend the wheel bearing life, but also reduce the possibility of any high frequency structural vibrations to influence the hi-resolution imaging. Fast slew manoeuvres enable amongst other advantages the possibility of stereo imaging and pointing of the propulsion thrusters during orbit control operations.

The Y-momentum stabilisation mode requires less satellite resources (on-board computing and ADCS hardware) to maintain the satellite's nominal nadir pointing attitude. This control mode is therefore also used as the backup ADCS software task on a redundant OBC in case of software failure of the main ADCS OBC.

Orbit control experiments have not been completed by the time the paper was submitted. The first experiment planned will be to control UoSAT-12 into frozen-orbit conditions. A high fidelity orbit controller designed by Microcosm[10] will then be utilised to demonstrate autonomous constellation maintenance.

Acknowledgements

The authors would like to acknowledge the support from all of the UoSAT-12 team at SSTL and the contributions made by the academic staff at CSER in making this first Surrey minisatellite mission, fitted with advanced AODCS, a possibility and a success.

References

1. Martel F., P.K. Pal and M.Psiaki, "Active Magnetic Control System for Gravity Gradient Stabilized Spacecraft", Proceedings of the 2nd Annual AIAA/USU Conference on Small Satellites, Utah State University, September 1988.

2. Thomson W.T., "Spin Stabilization of Attitude against Gravity Torque", Journal of Astronautical Science, No.9, pp.31-33, 1962.

3. Steyn, W.H., "A Multi-Mode Attitude Determination and Control System for Small Satellites", Ph.D. Thesis (Engineering), University of Stellenbosch, December 1995.

4. Wertz, J.R., Spacecraft Attitude Determination and Control, D.Reidel Publishing Company, Boston USA, Reprint 1986.

5. Stickler, A.C. and K.T. Allfriend, "An Elementary magnetic Attitude Control System", AIAA Mechanics and Control of Flights Conference, Anaheim California, August 1974.

6. Gelb, A., Apllied Optimal Estimation, The M.I.T. Press, Cambridge Massachusetts, 11th Print 1989.

7. Steyn, W.H., "Near Minimum-Time Eigenaxis Rotation maneuvers using Reaction Wheels", Journal of Guidance, Control, and Dynamics, Vol.18, No.5, September-October 1995.

8. Wie B., H.Weiss and A.Arapostathis, "Quaternion Feedback Regulator for Spacecraft Eigenaxis Rotations", Journal of Guidance, Control, and Dynamics, Vol.12, No.3, May-June 1989.

9. Palmer, P.L., S.J. Aarseth, S. Mikkola and Y. Hashida, "High Precision Integration Methods for Orbit Modelling", accepted for publication in Journal of Astronautical Sciences, 1999.

10. Königsmann, H.J., J.T. Collins, S Dawson and J.R.Wertz, "Autonomous Orbit Maintenance System", Acta Astronautica, Vol.39,No.9-12, 1996.